



Contents lists available at ScienceDirect

## Quaternary Science Reviews

journal homepage: [www.elsevier.com/locate/quascirev](http://www.elsevier.com/locate/quascirev)

## Glacial–interglacial and millennial-scale variations in the atmospheric nitrous oxide concentration during the last 800,000 years

Adrian Schilt<sup>a,b,\*</sup>, Matthias Baumgartner<sup>a,b</sup>, Thomas Blunier<sup>c</sup>, Jakob Schwander<sup>a,b</sup>, Renato Spahni<sup>a,b</sup>, Hubertus Fischer<sup>a,b</sup>, Thomas F. Stocker<sup>a,b</sup>

<sup>a</sup> Climate and Environmental Physics, Physics Institute, University of Bern, Sidlerstrasse 5, CH-3012 Bern, Switzerland

<sup>b</sup> Oeschger Centre for Climate Change Research, University of Bern, CH-3012 Bern, Switzerland

<sup>c</sup> Centre for Ice and Climate, Niels Bohr Institute, University of Copenhagen, Juliane Maries Vej 30, DK-2100 Copenhagen, Denmark

## ARTICLE INFO

## Article history:

Received 22 December 2008

Received in revised form

26 March 2009

Accepted 29 March 2009

Available online xxx

## ABSTRACT

We present records of atmospheric nitrous oxide obtained from the ice cores of the European Project for Ice Coring in Antarctica (EPICA) Dome C and Dronning Maud Land sites shedding light on the concentration of this greenhouse gas on glacial–interglacial and millennial time scales. The extended EPICA Dome C record covers now all interglacials of the last 800,000 years and reveals nitrous oxide variations in concert with climate. Highest mean interglacial nitrous oxide concentrations of 280 parts per billion by volume are observed during the interglacial corresponding to Marine Isotope Stage 11 around 400,000 years before present, at the same time when carbon dioxide and methane reach maximum mean interglacial concentrations. The temperature reconstruction at Dome C indicates colder interglacials between 800,000 and 440,000 years before present compared to the interglacials of the last 440,000 years. In contrast to carbon dioxide and methane, which both respond with lower concentrations at lower temperatures, nitrous oxide shows mean interglacial concentrations of 4–19 parts per billion by volume higher than the preindustrial Holocene value during the interglacials corresponding to Marine Isotope Stage 9–19. At the end of most interglacials, nitrous oxide remains substantially longer on interglacial levels than methane. Nevertheless, nitrous oxide shows millennial-scale variations at the same time as methane throughout the last 800,000 years. We suggest that these millennial-scale variations have been driven by a similar mechanism as the Dansgaard/Oeschger events known from the last glacial. Our data lead to the hypothesis that emissions from the low latitudes drive past variations of the atmospheric nitrous oxide concentration.

© 2009 Elsevier Ltd. All rights reserved.

### 1. Introduction

Nitrous oxide (N<sub>2</sub>O) is a well-mixed trace gas in the atmosphere that contributes substantially to the greenhouse effect. Its atmospheric concentration increased from a preindustrial value of about 265 parts per billion by volume (ppbv) (Flückiger et al., 2002) to a present-day value of 319 ppbv (Forster et al., 2007) due to anthropogenic emissions from agriculture, burning of fossil fuels and biomass, as well as industrial processes.

The preindustrial N<sub>2</sub>O source mainly results from nitrification and denitrification and is estimated at  $11 \times 10^{12}$  g of nitrogen per year (11 TgN/yr) (Kroeze et al., 1999). About two-thirds of these natural N<sub>2</sub>O emissions stem from soils, about one-third can be

attributed to marine emissions. The geographical distribution of the soil N<sub>2</sub>O source reveals a predominance of the tropics, where soil moisture conditions, temperature and high input of organic matter lead to favourable conditions for N<sub>2</sub>O emissions (Bouwman et al., 1993; Potter et al., 1996). In the ocean, N<sub>2</sub>O emissions are highest between 40 and 60 °S, but substantial emissions also stem from other latitudes especially from equatorial and coastal upwelling regions and the Arabian Sea (Nevison et al., 1995; Bange et al., 1996). Overall, 72% of terrestrial and 41% of marine N<sub>2</sub>O emissions are allocated to the latitudinal band between 30 °N and 30 °S (Nevison et al., 1995; Potter et al., 1996). The main sink of N<sub>2</sub>O is its decomposition by photodissociation (90%), followed by chemical reactions with excited oxygen (10%) (Minschwaner et al., 1998). Both these processes take place in the stratosphere. N<sub>2</sub>O has an atmospheric life time of about 120 years (Volk et al., 1997).

During the last 800,000 years (800 kyr), Earth's climate fluctuated between warm interglacials and cold glacials with the strongest periodicity around 100 kyr (Lisiecki and Raymo, 2005). Compared to

\* Corresponding author. Climate and Environmental Physics, Physics Institute, University of Bern, Sidlerstrasse 5, CH-3012 Bern, Switzerland. Tel.: +41 31 6314476; fax: +41 31 6318742.

E-mail address: [schilt@climate.unibe.ch](mailto:schilt@climate.unibe.ch) (A. Schilt).

the last millennium, Antarctic surface temperatures have been 10.3 °C colder during the coldest glacials and up to 4.5 °C warmer during the warmest interglacials (Jouzel et al., 2007). These climate variations affect the atmospheric N<sub>2</sub>O concentration, as revealed by reconstructions from ice cores covering the last 650 kyr (Spahni et al., 2005). On glacial–interglacial time scales, N<sub>2</sub>O responds with elevated concentrations during warm periods and reduced concentrations during cold periods (Fig. 1) (Flückiger et al., 1999; Spahni et al., 2005). On millennial time scales, fast increases of Greenland surface temperature of up to 15 °C are reconstructed during the last glacial (Huber et al., 2006). These millennial-scale variations, known as Dansgaard–Oeschger (DO) events, are accompanied by large increases in the methane (CH<sub>4</sub>) but also N<sub>2</sub>O concentrations. The CH<sub>4</sub> increases are in phase with or slightly lagging the temperature rises. However, at least for long-lasting events, the N<sub>2</sub>O increases start substantially before the onset of the rapid warming in the northern hemisphere (Flückiger et al., 1999, 2004).

Understanding of natural mechanisms leading to changes in global inventories of greenhouse gases in the past is crucial to determine the interaction of their atmospheric concentrations and global warming, and hence the radiative forcing in the future. In the following, we present and discuss N<sub>2</sub>O records measured along two different ice cores from Antarctica, providing further insight into glacial–interglacial and millennial-scale N<sub>2</sub>O variations back to 800 kyr before present (BP).

## 2. Method and data records

### 2.1. Measurement system

N<sub>2</sub>O is measured at the University of Bern on the same polar ice samples as CH<sub>4</sub>. The air is extracted from samples of about 40 g of ice with a melt-freezing technique and then analysed by gas chromatography. Two standard gases with N<sub>2</sub>O concentrations of

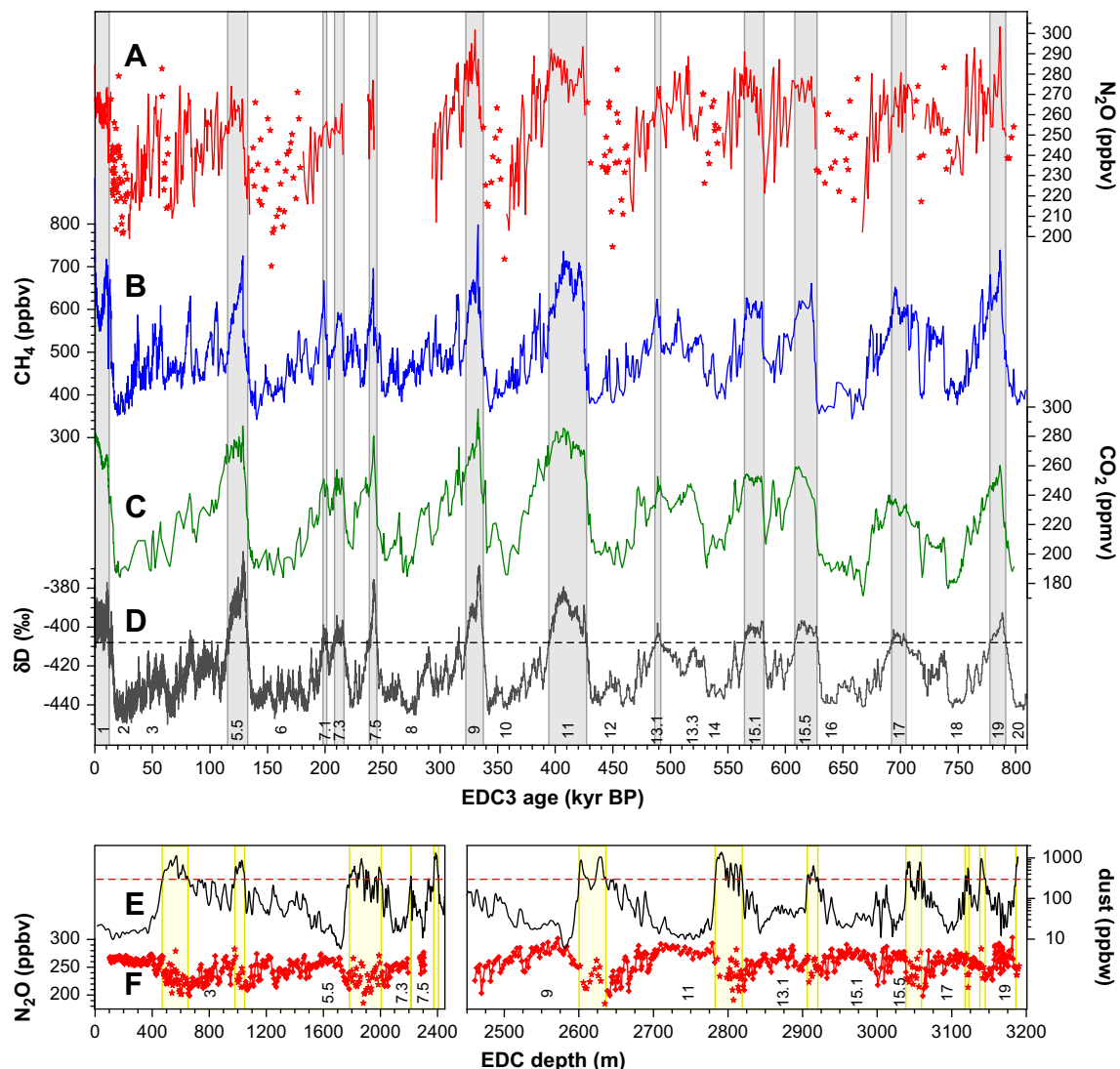


**Fig. 1.** Overview of reconstructed greenhouse gas concentrations from Antarctic ice cores. (A) Red: EDC N<sub>2</sub>O (Flückiger et al., 2002; Stauffer et al., 2002; Spahni et al., 2005 and new data). Stars denote values affected by artefacts (see dust and N<sub>2</sub>O records on the depth scale on the bottom panel). (B) Blue: EDC CH<sub>4</sub> (Monnin et al., 2001; Flückiger et al., 2002; Spahni et al., 2003; Spahni et al., 2005; Louergue et al., 2008). (C) Green: Vostok CO<sub>2</sub> (Petit et al., 1999) between 20 and 390 kyr BP, EDC CO<sub>2</sub> (Monnin et al., 2001; Monnin et al., 2004; Siegenthaler et al., 2005; Lüthi et al., 2008) elsewhere. (D) Dark grey: EDC  $\delta D$  (Jouzel et al., 2001; Jouzel et al., 2007). Grey shaded areas mark interglacials ( $\delta D > -408\text{‰}$  as highlighted by the dashed black line). N<sub>2</sub>O, CH<sub>4</sub>, CO<sub>2</sub> and  $\delta D$  are plotted on the EDC3 time scale (Louergue et al., 2007; Parrenin et al., 2007). (E) Black: EDC dust (Lambert et al., 2008), smoothed spline with a cutoff period of 2000 years (Enting, 1987). Yellow shaded areas mark depth intervals with dust concentrations above the threshold of 300 ppbw (dashed red line). (F) Red: EDC N<sub>2</sub>O, measurements made on ice with dust concentrations above the threshold are marked as values affected by artefacts (stars). Numbers denote MIS.

201 and 304 ppbv are used for calibration of an electron capture detector (ECD) and a thermal conductivity detector (TCD). Cross-checking with the standard gases CA04556, CA04565 and CA04561 showed that measurements calibrated on our scale are about 3.9% higher than they would be on the CMDL83 scale. Details about the measurement system and the calculation of the measurement error ( $1\sigma$ ), which averages to 4.1 ppbv over the records presented here, are given by Flückiger et al. (2004). Usually, one measurement is performed for each depth level. The interpretation of  $N_2O$  records requires some precautions, since  $N_2O$  concentrations measured along ice cores can be affected by in situ production of  $N_2O$  in the ice. These artefacts are discussed in Section 3.

## 2.2. Records

First, we analysed samples at 272 different depth levels along the whole ice core of the European Project for Ice Coring in Antarctica (EPICA) Dronning Maud Land (EDML, 75°00' S, 00°04' E) site. The artefact-free part of the EDML record covers the Holocene, parts of the last transition and glacial period, as well as the time interval between 134 and 69 kyr BP including Marine Isotope Stage (MIS) 5. The mean time resolution on the EDML1 time scale (Loulergue et al., 2007) is 250 years for the Holocene and 530 years for the rest of the record. Second, we extended the EPICA Dome C (EDC, 75°06' S, 123°21' E)  $N_2O$  record presented by Spahni et al. (2005) with new measurements at 293 different depth levels. With these new measurements over MIS 7.5, 9, 11, 17 and 19, the EDC  $N_2O$  record covers now (after removing all depth intervals subject to artefacts) 65% of the last 800 kyr including all interglacials back to this age. The mean time resolution of the new data on the EDC3 time scale (Loulergue et al., 2007) is 640 years for MIS 7.5 and MIS 9, 880 years for MIS 11 and 970 years for MIS 17–19.

## 3. Reliability of $N_2O$ records

As observed along other ice cores from Greenland and Antarctica (Flückiger et al., 1999; Sowers, 2001; Spahni et al., 2005) the  $N_2O$  measurements presented here are partly disturbed by artefacts. These artefacts originate from in situ production of  $N_2O$  in the ice and lead to values above the atmospheric concentration at that time. Although different mechanisms could lead to a surplus of  $N_2O$  in the ice, evidence is growing that microbial activity is responsible for the in situ production. It has been demonstrated in a lab experiment that ammonia-oxidizing bacteria are able to produce  $N_2O$  in ice at temperatures as low as  $-32^\circ\text{C}$  (Miteva et al., 2007). In addition,  $N_2O$  artefacts along the Vostok ice core seem to occur in ice with elevated levels of bacterial cells (Abyzov et al., 1998; Sowers, 2001).

Along the EDC ice core back to 650 kyr BP Spahni et al. (2005) observed unusually high concentrations and a large scatter for measurements made on ice with elevated dust concentrations, suggesting that bacteria are transported to Antarctica by the same pathway as dust. Thus, they excluded all  $N_2O$  concentrations measured on ice samples with dust concentrations above an empirical threshold of 300 parts per billion by weight (ppbw) from the atmospheric record. The availability of two overlapping  $N_2O$  records stemming from different ice cores (EDML and EDC) with different dust levels provides us with the opportunity to ascertain the atmospheric signal back to 140 kyr BP. At the same time, we are able to verify the dust criterion applied by Spahni et al. (2005). Because  $N_2O$  is globally well mixed, the EDML and EDC  $N_2O$  records should coincide in time intervals where no artefacts disturb the atmospheric signal.

Fig. 2 shows the EDML and EDC  $N_2O$  records back to 140 kyr BP, plotted on the synchronised EDML1 and EDC3 time scales

(Loulergue et al., 2007), respectively. Dust concentrations measured along the two ice cores (EPICA community members, 2006; Lambert et al., 2008) are plotted on the gas time scales as well ensuring that  $N_2O$  and dust measurements plotted at the same age stem from the same depth. We determine the agreement between the EDML and EDC  $N_2O$  records calculating a residual, which is defined as the difference between smoothed splines according to Enting (1987) (cutoff period of 3000 years) fitted through the data. In agreement with the dust criterion, no obvious correlation between the two records exists during intervals where at least one ice core shows dust concentrations above the threshold of 300 ppbw (yellow shaded areas in Fig. 2). During these time intervals the residual indicates differences between the EDML and EDC records of up to 60 ppbv. Even though some of the measurements marked as affected by artefacts might reflect atmospheric concentrations, we see no way to separate the atmospheric signal from the values affected by artefacts in these time intervals with the current time resolution. In intervals where the dust criterion suggests atmospheric signals for both, the EDML and EDC records, the two  $N_2O$  signals show the same shape on glacial–interglacial as well as on millennial time scales.

Even though the consistency between the EDML and EDC records is unambiguous during the Holocene (back to 14 kyr BP) as expressed by an absolute value of the mean of the residual of  $-0.6$  ppbv (SD: 1.5 ppbv), there are some disagreements between the two records for measurements rated as atmospheric concentrations by the dust criterion during MIS 5 (135–70 kyr BP). During this time interval the mean of the residual is 7.0 ppbv (SD: 2.1 ppbv) with slightly higher concentrations in the EDML compared to the EDC record.

In addition to inaccuracies in the time scales, a production of  $N_2O$  in ice with a dust concentration lower than 300 ppbw could also contribute to the observed difference between the EDML and EDC  $N_2O$  records during MIS 5. Since dust concentrations are generally higher at EDML than at EDC, an increasing in situ  $N_2O$  production concurrent with increasing dust concentrations would lead to higher  $N_2O$  concentrations measured along the EDML ice core compared to the EDC ice core. This is in agreement with our observations during MIS 5, where the EDML record not only shows higher values compared to the EDC record but where the maxima in the residual also coincide to a certain extent with the maxima in the difference between EDML and EDC dust concentrations. Since the EDML and EDC  $N_2O$  records of the last 2000 years are in good agreement with direct atmospheric measurements and with measurements in ice and firn air from Law Dome (Meure et al., 2006 and references therein), there is no indication for a contamination of the late Holocene  $N_2O$  records.

We check the possibility of a systematic drift in our measurement system by a total of 74 remeasurements along the EDC ice core covering previously published time intervals, namely the Holocene, MIS 3, 5 and 15 (Flückiger et al., 2002; Stauffer et al., 2002; Spahni et al., 2005) (Fig. 3). In order to correct for a systematic offset, which occurred around the year 2003 likely due to a shift in our standard gases, we add 10 ppbv to all subsequently measured  $N_2O$  concentrations along the EDC and the (whole) EDML ice cores. Spahni et al. (2005) determined this offset correction by resampling EDC Holocene ice and by comparing the EDML Holocene record with the earlier results from the EDC ice core (see supporting online material of Spahni et al. (2005) for more details). Fig. 3 illustrates the 95% confidence intervals of the median of the differences between the EDC remeasurements and the earlier record. For the Holocene, MIS 5 and 15, the remeasurements are statistically indistinguishable from the earlier record. For MIS 3, the median of the differences between remeasurements and the earlier record is 12.5 ppbv. However, those earlier measurements for MIS 3

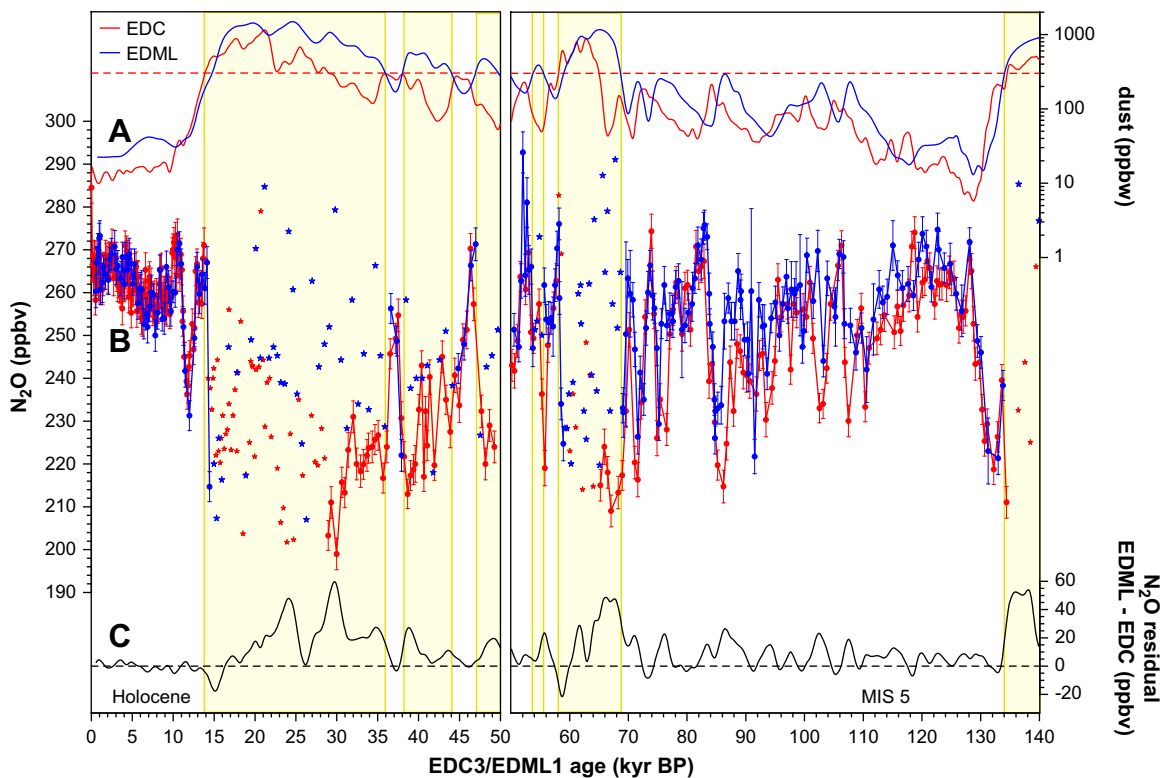


**Fig. 2.** Comparison of EDML and EDC  $N_2O$  and dust records. (A) Blue: EDML dust (EPICA community members, 2006). Red: EDC dust (Lambert et al., 2008). Shown are smoothed splines according to Enting (1987) with a cutoff period of 2000 years. The red dashed line shows the concentration threshold of 300 ppbw. (B) Blue: newly measured EDML  $N_2O$  on the EDML1 time scale (Loulergue et al., 2007). Red: EDC  $N_2O$  (Flückiger et al., 2002; Stauffer et al., 2002; Spahni et al., 2005) on the EDC3 time scale (Loulergue et al., 2007). Measurements stemming from ice with dust concentrations above the threshold of 300 ppbw are marked as affected by artefacts (stars). (C) Residual, defined by the difference between smoothed splines (cutoff period of 3000 years) through EDML and EDC  $N_2O$  records. Dust data are plotted on the gas time scales. Accordingly, gas and dust measurements with the same age on this plot have been measured at equal depth levels. Intervals where at least one record shows dust concentrations above the threshold of 300 ppbw are marked with yellow shaded areas.

did not reveal the expected concentration increases in response to the DO events 6 and 7, pointing to potential instabilities in the measurement system at the time of the earlier measurements. Furthermore, the measurements from this time interval have been

made on glacial ice with higher amounts of impurities and might therefore be partly affected by in situ production of  $N_2O$  possibly causing large variations in even neighbouring ice samples. Except for the few data over MIS 3, the remeasurements along the EDC ice

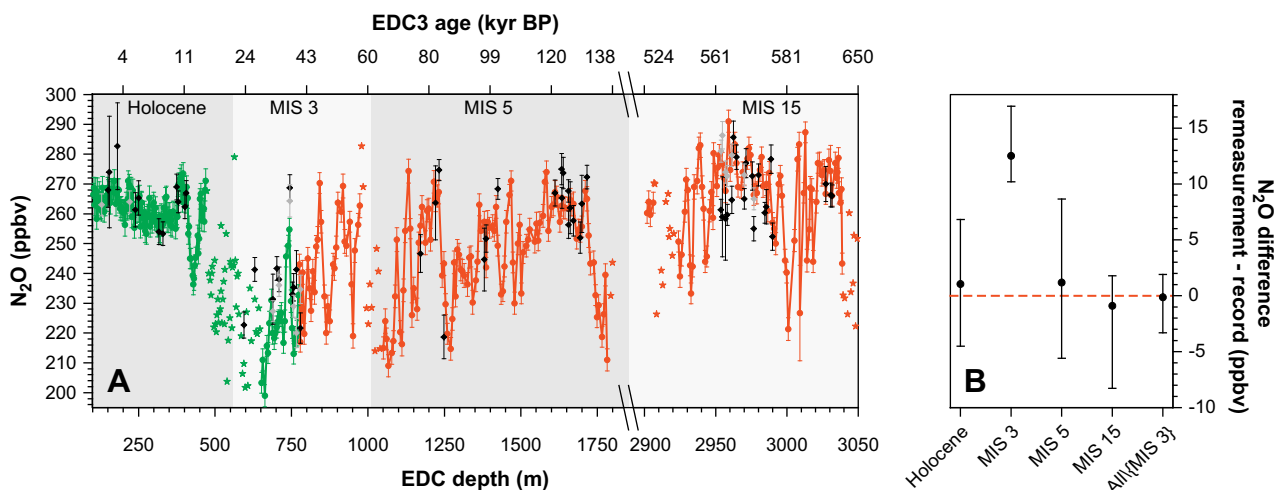


**Fig. 3.**  $N_2O$  remeasurements along the EDC ice core on a depth scale. (A) Green: EDC  $N_2O$  (Flückiger et al., 2002; Stauffer et al., 2002; Spahni et al., 2005), measured in the years 1998–2001, no offset correction applied. Red: EDC  $N_2O$  (Spahni et al., 2005), measured in the years 2003–2005, corrected by +10 ppbv. Black diamonds: EDC  $N_2O$  remeasurements, measured in the year 2006, corrected by +10 ppbv. Grey diamonds: EDC  $N_2O$  remeasurements, measured in the year 2008, corrected by +10 ppbv. EDC3 ages (Loulergue et al., 2007) are indicated on the top x-axis. (B) Median with 95% confidence intervals of the differences between remeasurements and earlier record calculated for the different time intervals and for all remeasurements (excluding MIS 3, see Section 3) together. The confidence intervals are calculated assuming a binomial distribution of the signs of the differences. The two remeasurements with higher concentrations and large error bars standing out of the Holocene record as well as the low remeasurements during MIS 15 are likely affected by a systematic error during the measurement process. Although second remeasurements revealed the expected values, the first measurements are taken into account for the calculation of the confidence intervals.

core agree well with earlier measurements and confirm the offset correction of +10 ppbv (Fig. 3).

While noting that a small in situ production leading to slightly elevated  $N_2O$  concentrations cannot completely be excluded even for samples with a dust concentration below 300 ppbw, for instance because of possible concentrating of nutrients and bacteria at grain boundaries, we continue to use the dust criterion to separate values affected by artefacts from the atmospheric signal for the EDML as well as for the EDC record back to 800 kyr BP. The separation of  $N_2O$  values affected by artefacts for the EDML and EDC records is shown in Figs. 1 and 2. We are aware that the dust criterion as applied to the EDC and EDML ice cores is an empirical approach and application to other ice cores may be problematic. Indeed, measurements along the ice core of the Greenland Ice Sheet Project Two (GISP2) revealed high microbial concentrations coinciding with  $N_2O$  artefacts in ice with low dust concentrations (Rohde et al., 2008). Thus, the dust criterion as used for the EDML and EDC  $N_2O$  records cannot be applied to  $N_2O$  records from Greenland, as also revealed by comparing highly resolved  $N_2O$  measurements along the ice core of the North Greenland Ice Core Project (NGRIP) with the dust concentration of the measured samples (see Flückiger et al., 2004).

Although the empirical dust criterion seems to work for most data points measured along the ice cores presented here, future measurements of the microbial concentrations are needed to investigate the correlation of microbial concentrations with dust concentrations and  $N_2O$  artefacts. Such continuous measurements of the microbial concentration promise to become a tool for a reliable separation of  $N_2O$  values affected by artefacts from the atmospheric records (Rohde et al., 2008).

## 4. Results

### 4.1. EDML

Our measurements along the EDML ice core provide a second precise  $N_2O$  record back to 140 kyr BP, allowing a direct comparison with the EDC record (Flückiger et al., 2002; Stauffer et al., 2002; Spahni et al., 2005). For the Holocene, our new measurements confirm the observations made by Flückiger et al. (2002): after a decrease in the early Holocene and minimum concentrations

between 8 and 6 kyr BP (<260 ppbv),  $N_2O$  slowly increases to its preindustrial concentration of about 265 ppbv. The drop of about 30 ppbv in the EDML  $N_2O$  record during the Younger Dryas (YD) is in good agreement with the EDC record (Fig. 2). For the last glacial maximum, neither the EDML nor the EDC record provide atmospheric  $N_2O$  concentrations due to the artefacts. During MIS 5, the EDML and EDC records show mostly synchronous variations on glacial–interglacial time scales as well as in response to millennial-scale variations.

### 4.2. EDC

For the last 800 kyr, Fig. 1 gives an overview of the atmospheric concentrations of the greenhouse gases  $N_2O$  (Flückiger et al., 2002; Stauffer et al., 2002; Spahni et al., 2005 and new data),  $CH_4$  (Monnin et al., 2001; Flückiger et al., 2002; Spahni et al., 2003; Spahni et al., 2005; Loulergue et al., 2008) and carbon dioxide ( $CO_2$ ) (Petit et al., 1999; Monnin et al., 2001; Monnin et al., 2004; Siegenthaler et al., 2005; Lüthi et al., 2008), as well as of deuterium ( $\delta D$ ) (Jouzel et al., 2001, 2007), which is a proxy for Antarctic temperature. In addition, Fig. 4 shows in detail the newly measured EDC  $N_2O$  data (together with  $CH_4$  and  $\delta D$ ) covering MIS 9–11 and MIS 17–19.

As  $CO_2$  and  $CH_4$ ,  $N_2O$  generally varies in line with climate on orbital time scales, revealing high concentrations during interglacials and low concentrations during glacials.  $N_2O$  shows highest concentrations of 286 ppbv (mean over at least 7 kyr) during MIS 11. This concentration is considerably higher than the preindustrial concentration of 265 ppbv, but substantially lower than the present-day concentration of 319 ppbv (Forster et al., 2007). During MIS 11, the  $N_2O$  record exceeds the mean Holocene concentration of 261 ppbv for about 32 kyr. Further, the low  $CO_2$  concentration of 172 parts per million by volume (ppmv) reported at 667 kyr BP (Lüthi et al., 2008) falls together with lowest atmospheric  $N_2O$  concentrations (202 ppbv) measured along the EDC ice core. However, it is not possible to claim this  $N_2O$  value to be unusually low, since our record does not allow a complete insight into glacial  $N_2O$  concentrations due to the problem of artefacts.

Along the EDC ice core we define interglacials as time intervals where  $\delta D$  exceeds  $-408\text{‰}$ . Although this choice is somewhat arbitrary, it represents an objective definition of interglacials and ensures that the Holocene as well as the time intervals

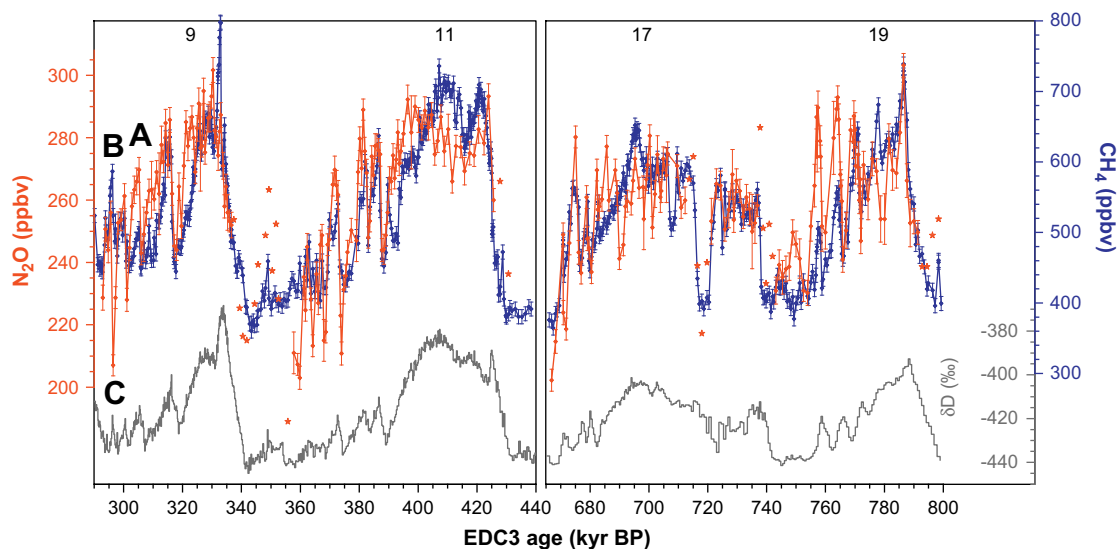


**Fig. 4.** EDC  $N_2O$ ,  $CH_4$  and  $\delta D$  records covering MIS 9, 11, 17 and 19. (A) Red: newly measured EDC  $N_2O$ . Stars denote values affected by artefacts. (B) Blue: EDC  $CH_4$  (Spahni et al., 2005; Loulergue et al., 2008). (C) Dark grey: EDC  $\delta D$  (Jouzel et al., 2007). The x-axis is broken between MIS 11 and 17. Data are plotted on the EDC 3 time scale (Loulergue et al., 2007; Parrenin et al., 2007).

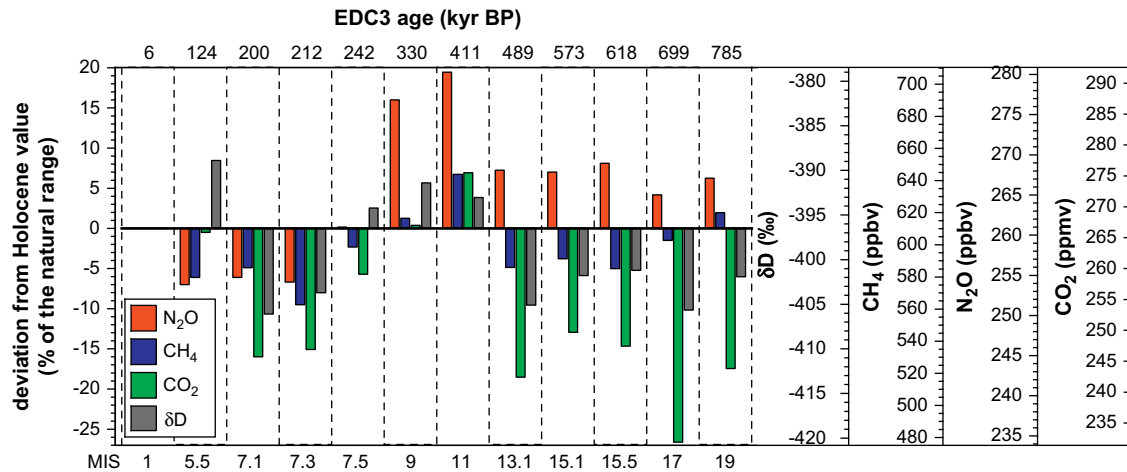


**Fig. 5.** Mean values of N<sub>2</sub>O (red), CH<sub>4</sub> (blue), CO<sub>2</sub> (green) and δD (dark grey) during the interglacials (δD > -408‰) of the last 800 kyr. Values are given on an absolute scale (right y-axis) and as deviation from the mean Holocene value in percent of the natural range (left y-axis). Interglacials are denoted on the bottom x-axis, the mean age of the interglacials (EDC3 time scale) on the top x-axis. See caption of Fig. 1 for references.

corresponding to MIS 5.5, 7.1, 7.3, 7.5, 9, 11, 13.1, 15.1, 15.5, 17 and 19 are identified as interglacials (grey shaded areas in Fig. 1). For every interglacial we calculate mean values of N<sub>2</sub>O, CH<sub>4</sub>, CO<sub>2</sub> and δD. On the bar plot in Fig. 5 the mean interglacial values are shown as the relative deviation from the mean Holocene value in percent of the natural range of each component (which is set to 100 ppbv for N<sub>2</sub>O, 500 ppbv for CH<sub>4</sub>, 130 ppmv for CO<sub>2</sub> and 90‰ for δD). This allows us to put different components on a common scale for a direct comparison.

Highest mean interglacial N<sub>2</sub>O concentrations are observed during MIS 11 (280 ppbv), followed by MIS 9 (277 ppbv) and MIS 15.5 (269 ppbv). The highest mean interglacial concentration of N<sub>2</sub>O, observed during MIS 11, coincides with highest mean interglacial concentrations of CO<sub>2</sub> and CH<sub>4</sub> indicating that climate conditions have been favourable for strong emissions for all greenhouse gases at this time.

Despite the coincidence of maximum mean interglacial concentrations of N<sub>2</sub>O, CH<sub>4</sub> and CO<sub>2</sub> during MIS 11, large differences in the response of the greenhouse gases to changing climate are observed during the last 800 kyr. The EDC δD record indicates that Antarctic temperatures during interglacials before 440 kyr BP have been lower than those of interglacials of the past four climatic cycles (EPICA community members, 2004; Jouzel et al., 2007). Apart from the short and relatively cool interglacials MIS 7.1 and 7.3, CO<sub>2</sub> clearly follows this trend and shows lower concentrations during the interglacials between 800 and 440 kyr BP compared to the interglacials of the last 440 kyr. With MIS 19 as an exception, maximum interglacial CH<sub>4</sub> concentrations behave the same way, however, the pattern for CH<sub>4</sub> becomes less clear when mean interglacial concentrations are considered (Fig. 5). In contrast to CO<sub>2</sub> and CH<sub>4</sub>, N<sub>2</sub>O does not respond to the shift in temperatures and shows higher concentrations during MIS 9–19 compared to MIS 1–7. A different response of N<sub>2</sub>O (compared to CO<sub>2</sub> and CH<sub>4</sub>) to Antarctic temperature is also visible when comparing MIS 5.5 and 9. These two interglacials show quite similar δD, CO<sub>2</sub> and CH<sub>4</sub> records, while the mean interglacial concentration of N<sub>2</sub>O is about 23 ppbv higher during MIS 9 compared to MIS 5.5 (Figs. 5 and 6). A valid question to be raised in this context concerns the potential of a slow in situ production of N<sub>2</sub>O being able to influence the older interglacials (preserved in warmer ice) more strongly than the younger ones. While this cannot be completely ruled out, it appears to be unlikely because there exists no long-term trend in N<sub>2</sub>O concentrations with age of the ice. In fact, MIS 13–19 all show very

similar concentrations which are substantially reduced compared to the much younger MIS 11 despite somewhat higher dust concentrations in the older interglacials. Note also that the dust levels in all interglacials are still well below the threshold of 300 ppbv. For instance during MIS 11, dust levels are on the order of the Holocene concentration, therefore it is unlikely that the high N<sub>2</sub>O concentrations during MIS 11 are caused by in situ N<sub>2</sub>O production in the ice. Further, the variability of the N<sub>2</sub>O measurements (in this context defined as the standard deviation of the difference between individual data points and a spline with a cutoff period of 5000 years calculated through the data records) remains roughly constant (between 3.8 and 6.4 ppbv) and does not increase in the older interglacials. Such increase would be a likely result of slow in situ production or a dependency on ice temperature (see

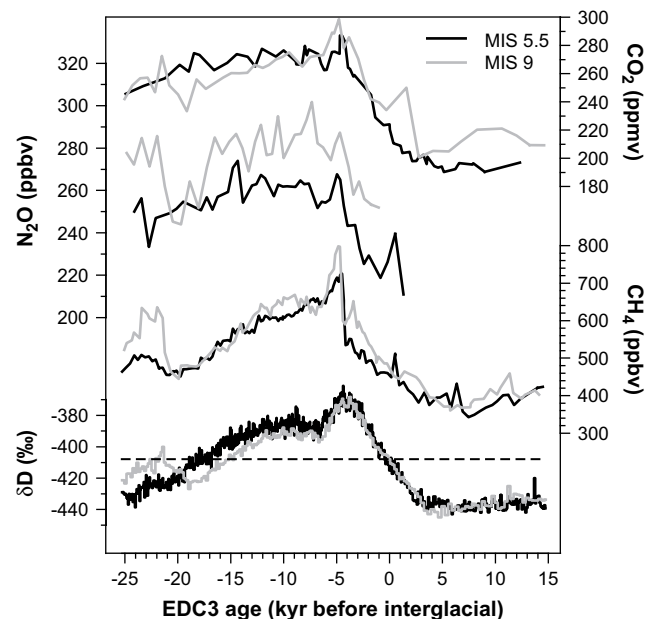


**Fig. 6.** Comparison of Vostok CO<sub>2</sub>, EDC N<sub>2</sub>O, EDC CH<sub>4</sub> and EDC δD during MIS 5.5 (black lines) and 9 (grey lines). Data are shown on the EDC3 time scale and the records are aligned by synchronisation of the start time of MIS 5.5 and 9. While CO<sub>2</sub>, CH<sub>4</sub> and δD show quite similar records during MIS 5.5 and 9, the N<sub>2</sub>O records differ substantially during these interglacials. See caption of Fig. 1 for references.

also Section 3). Nevertheless, we note that our observations, in particular the high  $N_2O$  concentrations during MIS 11 and during the interglacials between 800 and 440 kyr BP, will only be fully substantiated when similar results show up from other ice cores and when parallel measurements of  $N_2O$  isotopes and microbial concentrations become available.

#### 4.3. End of interglacials

A different behaviour of  $N_2O$  compared to  $CH_4$  further appears at the end of interglacials. Since  $N_2O$  and  $CH_4$  are measured on the same ice samples, the two records can be compared without any uncertainty in timing. At the end of interglacials,  $N_2O$  generally tends to remain substantially longer on the interglacial level than  $\delta D$  and  $CH_4$ , which start to decrease synchronously on glacial–interglacial time scales. The yellow areas in Fig. 7 clearly indicate these lags of  $N_2O$  with respect to  $\delta D$  and  $CH_4$  at the end of the interglacials MIS 5.5, 7.3, 9, 11, 15.1 and 15.5, where  $N_2O$  starts to decrease towards glacial values between 2 and 11 kyr later than  $CH_4$ . Very sparse data indicate an analogous lag of  $N_2O$  at the end of MIS 7.5 (Fig. 1). At the end of MIS 7.1 and 13.1 our data indicate a rather synchronous decrease of  $N_2O$  and  $CH_4$ . Also, at the end of MIS 17,  $N_2O$  and  $CH_4$  start to decrease around the same time, but  $N_2O$  then returns to interglacial levels for several thousand years, while  $\delta D$  and  $CH_4$  continue their steady decrease. Since the transition from MIS 19 to MIS 18 is interrupted by millennial-scale variations well represented in the  $N_2O$  record (see Section 5.2), it is difficult to define the time of the greenhouse gas concentration decrease at the end of MIS 19. However, as for all other interglacials

of the last 800 kyr, a decrease of  $N_2O$  prior to a decrease of  $CH_4$  and  $\delta D$  can be excluded.

To a certain degree,  $N_2O$  and  $CO_2$  vary in line at the end of interglacials. This is for example apparent during MIS 5.5, where  $\delta D$  and  $CH_4$  decrease while  $N_2O$  and  $CO_2$  remain on a stable level or during MIS 11, where  $\delta D$  and  $CH_4$  decrease while  $N_2O$  and  $CO_2$  increase.

## 5. Discussion

### 5.1. Possible dominance of $N_2O$ emissions from low latitudes

Our data demonstrate that the coupling to Antarctic temperature is less pronounced for  $N_2O$  than for  $CO_2$  and  $CH_4$  (Section 4.2), and that the decrease of  $N_2O$  lags the decrease of  $CH_4$  at the end of most interglacials (Section 4.3). As a possible explanation for these observations we hypothesise that on glacial–interglacial time scales  $N_2O$  emissions are mainly controlled by processes located in low latitudes, while  $CO_2$  and  $CH_4$  emissions are also modulated by processes located in high latitudes. Indeed, the Southern Ocean is considered as an important regulator of atmospheric  $CO_2$  (Köhler et al., 2005; Watson and Garabato, 2006), while  $CH_4$  emissions from wetlands located in high northern latitudes, although not reaching the magnitudes of tropical  $CH_4$  sources, contribute to the glacial–interglacial difference and especially to rapid  $CH_4$  variations (Dällenbach et al., 2000; Fischer et al., 2008).

At the glacial inception, when large ice sheets start to develop in the northern hemisphere, terrestrial greenhouse gas emissions from high latitudes are likely reduced at a time when emissions from low latitudes may still be on the interglacial level. The lag of

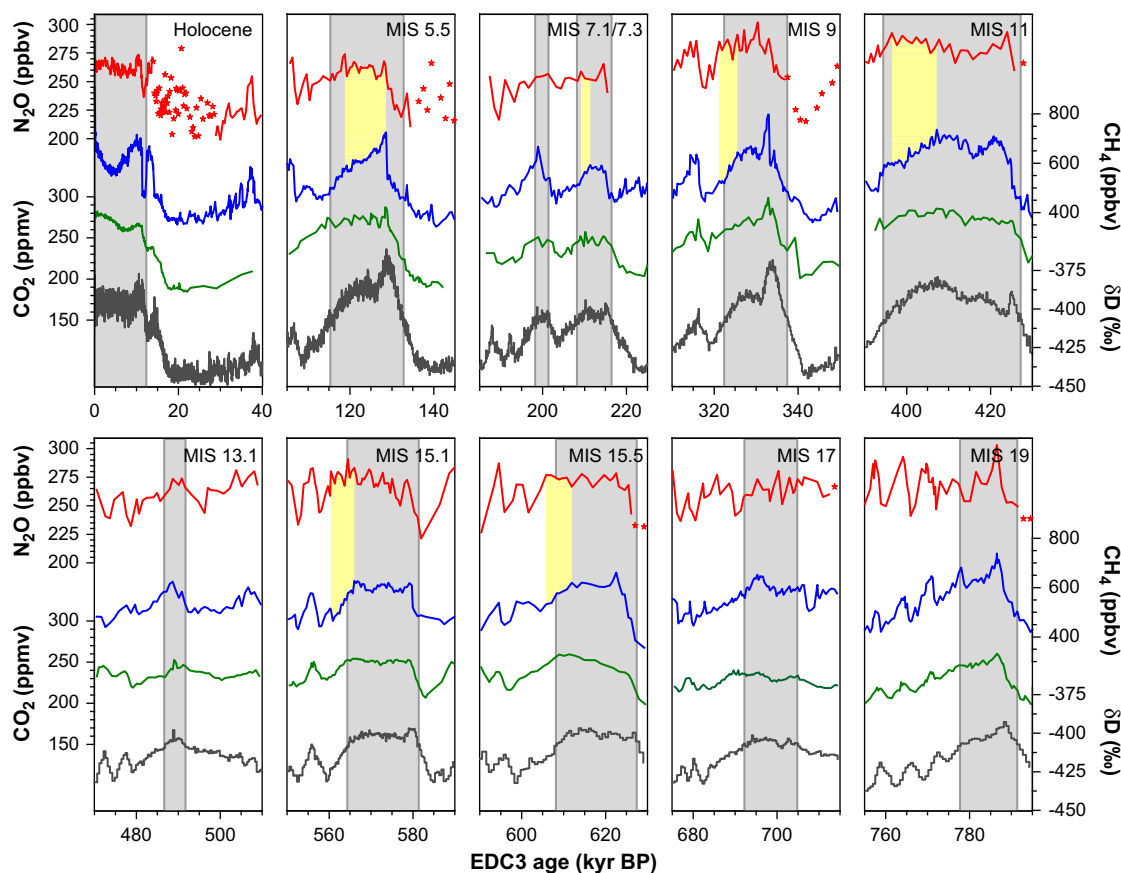


Fig. 7. Overview of  $N_2O$ ,  $CH_4$ ,  $CO_2$  and  $\delta D$  during interglacials of the last 800 kyr. Yellow areas indicate time intervals for which  $CH_4$  already started to decrease from interglacial to glacial values, while  $N_2O$  still remains on the interglacial level. See caption of Fig. 1 for colour codes and references.

the N<sub>2</sub>O decrease with respect to CH<sub>4</sub> at the end of interglacials could, thus, indicate that high latitudes are less important for N<sub>2</sub>O than for CH<sub>4</sub> emissions, in agreement with our hypothesis. We point out that the longer atmospheric life time of N<sub>2</sub>O compared to that of CH<sub>4</sub> is irrelevant on these time scales and cannot be used as an explanation for the observed lag of N<sub>2</sub>O.

Further, maximum N<sub>2</sub>O concentrations during millennial-scale variations (DO type events prior to the last glacial) often reach typical interglacial N<sub>2</sub>O values although temperatures ( $\delta D$ ) have already declined from full interglacial conditions (Fig. 1, Fig. 8 and Section 5.2) as for instance visible during the last glacial as well as during MIS 10 and 18. In contrast, maximum CH<sub>4</sub> concentrations during these variations are lower than typical interglacial values and, additionally, they decrease with decreasing temperature (and increasing ice volume). We suggest that extended ice sheets in the northern hemisphere prevent CH<sub>4</sub> from reaching interglacial levels during millennial-scale variations. The insensitivity of N<sub>2</sub>O maxima to the extent of ice sheets could be understood as a further indicator of a dominance of the low latitudes to global N<sub>2</sub>O emissions. However, the global ocean might also play an important role during millennial-scale variations, as discussed in Section 5.2.

The comparison of N<sub>2</sub>O and CO<sub>2</sub> at the end of MIS 5.5 and 11, where both gases still show interglacial concentrations while  $\delta D$  and CH<sub>4</sub> already decrease, further supports our low latitude hypothesis. Since during these time intervals CO<sub>2</sub> does not follow the Antarctic temperature and hence the accompanying changes in the Southern Ocean parallel to the expansion of sea-ice, CO<sub>2</sub> emissions from low latitudes could have played a dominant role. In the case CO<sub>2</sub> emissions from low latitudes are responsible for the observed trend, N<sub>2</sub>O emissions from the same geographical regions may have changed in concert with CO<sub>2</sub> emissions. If marine processes were entirely responsible for the observed changes in CO<sub>2</sub>, the ocean might play an important role for N<sub>2</sub>O as well. In the ocean, denitrification could account for a possible link between CO<sub>2</sub> and N<sub>2</sub>O emissions. On the one hand, high denitrification rates enhance the production of molecular nitrogen and N<sub>2</sub>O, which both escape into the atmosphere. On the other hand, low concentrations of fixed nitrogen (which can be a limiting factor for biomass production) reduce the biological carbon pump and less carbon is removed from the atmosphere and stored in the ocean. Thus, high denitrification rates could be responsible for high atmospheric N<sub>2</sub>O concentrations in line with high CO<sub>2</sub> concentrations (Meissner et al., 2005). However, a terrestrial release of carbon during the glacial inception could also contribute to the high atmospheric CO<sub>2</sub> levels.

### 5.2. DO-like events throughout the last 800 kyr

In addition to the considerable N<sub>2</sub>O variations between glacials and interglacials, the EDC record also reveals N<sub>2</sub>O concentration changes on millennial time scales. For the last glacial, N<sub>2</sub>O variations in response to the DO events 8, 9, 10, 11, 12, 19 and 20 have been documented with highly resolved records (Flückiger et al., 1999, 2004). During these events, the temperature recorded in Greenland ice cores as well as the CH<sub>4</sub> concentration changed rapidly (e.g. Huber et al., 2006). Further, ice cores from Antarctica demonstrate that a warming of the southern hemisphere preceded all DO events at least back to 50 kyr BP (EPICA community members, 2006). Regarding the response of N<sub>2</sub>O to DO events during the last glacial it was pointed out that the amplitudes increase with increasing durations of the events (Flückiger et al., 2004). This correlation between N<sub>2</sub>O amplitude and duration seems to be a general characteristic of DO events during the last glacial.

Our EDC N<sub>2</sub>O record covering the last 800 kyr reveals a maximum in the N<sub>2</sub>O concentration concomitant with every CH<sub>4</sub> millennial-scale variation associated with an Antarctic Isotope Maximum (Fig. 1). Despite the gaps in the N<sub>2</sub>O record as a consequence of artefacts and despite a possible lack of variations both in the CH<sub>4</sub> and N<sub>2</sub>O records due to the sometimes coarse time resolution, the synchrony of the N<sub>2</sub>O and CH<sub>4</sub> millennial-scale variations throughout the EDC record supports the reliability of the atmospheric N<sub>2</sub>O record on millennial time scales. Overall, 29 such millennial-scale variations with amplitudes between 21 and 53 ppbv and durations of a few hundred to several thousand years are identified.

The determination of amplitudes and durations of millennial-scale variations during the last 800 kyr allows a comparison with the DO events during the last glacial. As shown in Fig. 8, the amplitude of each millennial-scale N<sub>2</sub>O variation is calculated by subtracting the baseline from the maximum value reached during the variation, whereby the value of the baseline is given by linear interpolation of the local minima before and after the variation. Since CH<sub>4</sub> is strongly correlated to the temperature changes of the northern hemisphere (Brook et al., 1996) the duration of the variations is determined using the CH<sub>4</sub> record and is defined as the width at half amplitude. Because the variations sometimes consist of only a few data points we are aware that in particular the calculated N<sub>2</sub>O amplitudes could change by improving the time resolution of our record. Nevertheless, we are confident that the determined values allow a qualitative investigation of the relationship between amplitudes and durations of millennial-scale variations throughout the EDC record. Indeed, the comparison of N<sub>2</sub>O amplitudes and durations during the millennial-scale variations of the last 800 kyr reveals a statistically significant linear relationship (Fig. 9), analogous to the observations for selected DO events during the last glacial (Flückiger et al., 2004). It must be pointed out that for this comparison we ignored the DO events 5, 6 and 7, although the EDC N<sub>2</sub>O record is not disturbed by artefacts during the respective time interval according to the dust criterion. However, the record of this time interval does not show any variations in response to the DO events and conflicts with our remeasurements. We cannot rule out the possibility that the earlier N<sub>2</sub>O measurements for that time interval are compromised by bad data quality (see Section 3).

We state that amplitudes and durations of millennial-scale variations during the last 800 kyr as well as the relationship between these two parameters are consistent with DO events during the last glacial. This consistency supports the hypothesis that millennial-scale variations during the last glacial period and during earlier time intervals have been driven by the same mechanisms. In agreement with this result, Lüthi et al. (2008), who compared millennial-scale variations during MIS 18 with DO events during MIS 3, concluded that the bipolar seesaw (Stocker, 1998; Stocker and Johnsen, 2003; EPICA community members, 2006) has been active beyond the last glacial.

The question arises how these millennial-scale climate variations affect the emissions of N<sub>2</sub>O. The observed increase of the N<sub>2</sub>O amplitudes with increasing durations of the millennial-scale variations implies that the N<sub>2</sub>O production does not reach saturation in the course of these millennial-scale variations. Therefore, N<sub>2</sub>O emissions may have increased approximately linearly with increasing duration of the millennial-scale variations.

Since CH<sub>4</sub> is dominated by terrestrial sources and since millennial-scale climate variations lead to concomitant variations in both, the CH<sub>4</sub> and the N<sub>2</sub>O concentrations, terrestrial emissions may play an important role for N<sub>2</sub>O as well. CH<sub>4</sub> production prefers completely anaerobic conditions and, thus, soils with a water-filled pore space of 100%, while N<sub>2</sub>O is emitted from soils



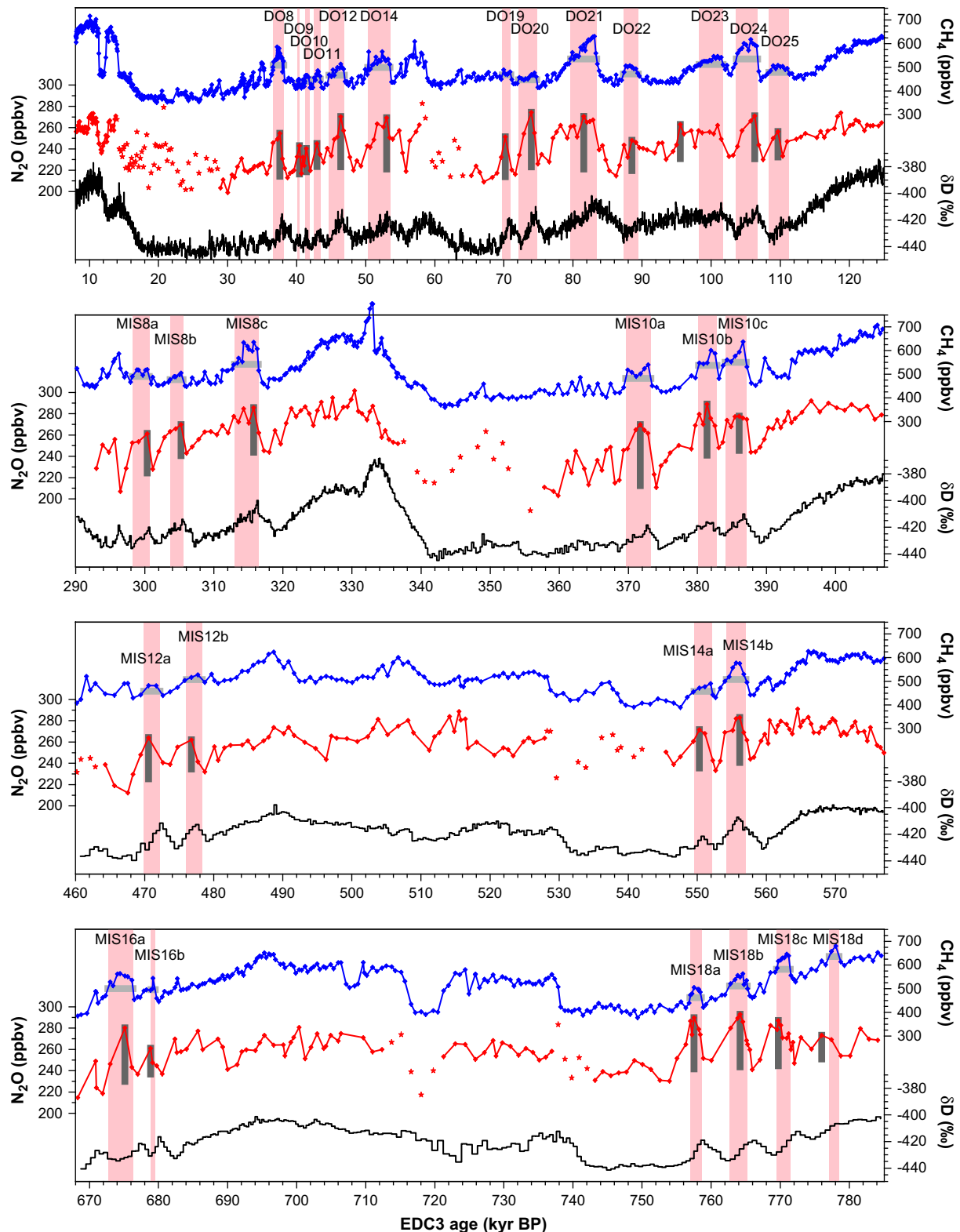


**Fig. 8.** Millennial scale events during the last 800 kyr. Blue line: EDC  $\text{CH}_4$ . Red line: EDC  $\text{N}_2\text{O}$ . Black line: EDC  $\delta\text{D}$ .  $\text{N}_2\text{O}$  amplitudes of millennial scale events are marked with vertical lines (dark grey). Durations of millennial scale events are marked with horizontal lines (light grey) and shaded with red areas. All records are plotted on the EDC3 time scale. See caption of Fig. 1 for references.

with 40–80% water-filled pore space (Davidson, 1991). This difference may account for different responses of the terrestrial  $\text{CH}_4$  and  $\text{N}_2\text{O}$  sources even in the case the sources are located in the same regions/latitudes and exposed to similar changes in

precipitation and temperature. However, it is not evident why  $\text{CH}_4$  emissions (only terrestrial) react immediately to climate variations, while terrestrial  $\text{N}_2\text{O}$  emissions should need thousands of years to adapt to a new climatic situation. Therefore, we conclude

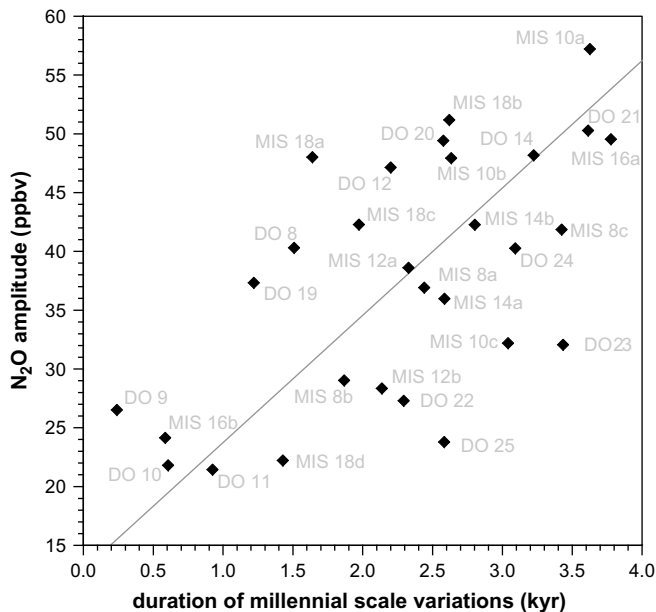


**Fig. 9.** Correlation between durations and  $N_2O$  amplitudes of 29 millennial-scale variations of the last 800 kyr. The amplitude is calculated by subtracting the baseline from the maximum value reached during the variation, whereby the value of the baseline is given by linear interpolation of the local minima before and after the variation. The duration is determined using the  $CH_4$  record and is defined as the width at half amplitude (see Fig. 8). The grey line indicates a two-sided regression.

that an important contribution of marine  $N_2O$  sources may also be required in order to explain the observed dependency of  $N_2O$  amplitude on the duration of the millennial-scale variations (see also discussion in Flückiger et al., 2004). Support for a marine contribution comes from a closer look at the millennial-scale variations which also reveals, besides the concomitant  $CH_4$  and  $N_2O$  variations, differences between the responses of the two greenhouse gases. For instance, highly resolved records show that  $N_2O$  starts to increase several hundred years before  $CH_4$  at the beginning of long-lasting DO events (Flückiger et al., 2004), a pattern which is hardly captured by the EDC record presented here given its mean time resolution of about 800 years. A recent model simulation suggests that changes in the Atlantic Meridional Overturning Circulation (AMOC) related to millennial-scale variations strongly affect the marine productivity and the oxygen content of the thermocline and, thus, marine  $N_2O$  emissions from the tropical Pacific, the northern Indian Ocean and elsewhere (Schmittner and Galbraith, 2008). The model reproduces the early increase of  $N_2O$  before the rapid temperature rise in Greenland, probably as the result of long-term adjustment of upper-ocean nitrate and oxygen inventories. Remarkably, the model further shows larger decreases of the  $N_2O$  concentration for longer-lasting stadials, supporting the idea that there is not enough time to reach the full amplitude and thus an equilibrium in the course of the millennial-scale variations. Schmittner and Galbraith (2008) note that the comparison of  $N_2O$  decrease and duration of the stadial should yield very similar results as the comparison of  $N_2O$  increase and duration of the interstadial. Thus, the model results are in good agreement with the observation that the  $N_2O$  amplitudes increase with increasing durations of millennial-scale variations (Fig. 9). Note that according to Schmittner and Galbraith (2008) the ocean is solely responsible for the complete amplitude of the observed changes in the  $N_2O$  concentration during millennial-scale variations. Their model does not include terrestrial  $N_2O$  changes. While a constancy of terrestrial  $N_2O$

emissions cannot be ruled out, it seems highly unlikely that terrestrial  $N_2O$  sources, which account for about two-thirds of the total  $N_2O$  emissions today, did not change at all when at the same time terrestrial  $CH_4$  emissions from boreal and tropical wetlands lead to substantial changes in the atmospheric  $CH_4$  concentration as well as in its interhemispheric gradient (Dällenbach et al., 2000).

## 6. Conclusion

Along the EDC  $N_2O$  record back to 800 kyr BP highest concentrations (observed during MIS 11) exceed the preindustrial Holocene value of 265 ppbv (Flückiger et al., 2002) by more than 20 ppbv, however, these values are still substantially lower than today's anthropogenic concentrations of 319 ppbv (Forster et al., 2007).

Our data suggest that low latitudes may have been the key region regarding changing emissions of  $N_2O$  on glacial–interglacial time scales. While  $CO_2$  and  $CH_4$  show lower concentrations during the colder interglacials between 800 and 440 kyr BP compared to the interglacials of the last 440 kyr,  $N_2O$  concentrations show increased levels. At the end of most interglacials,  $N_2O$  generally remains several thousand years longer on the interglacial level than  $CH_4$ , which starts to decrease synchronously with Antarctic temperature.

Millennial-scale  $N_2O$  variations throughout the entire last 800 kyr are consistent with  $N_2O$  variations observed in relation with the DO events documented during the last glacial. This supports the hypothesis that DO type events driven by deep water formation changes in the North Atlantic occurred also in previous glacials. It further suggests that these deep water changes have an influence on atmospheric  $N_2O$  levels either by concurrent changes in the terrestrial (low latitude) biosphere or by a direct change in the marine  $N_2O$  production (Schmittner and Galbraith, 2008).

Based on our records it is not possible to draw final conclusions of the underlying biogeochemical processes leading to the observed  $N_2O$  variations. However, the records presented here, together with future measurements of the  $N_2O$  concentration and its isotopic composition, provide a benchmark for model simulations.

## Acknowledgment

This work is a contribution to the European Project for Ice Coring in Antarctica (EPICA), a joint European Science Foundation/European Commission scientific program, funded by the European Commission and by national contributions from Belgium, Denmark, France, Germany, Italy, the Netherlands, Norway, Sweden, Switzerland and the United Kingdom. The main logistic support was provided by IPEV/PNRA (at Dome C) and AWI (at Dronning Maud Land). We thank the technical teams in the field and at the laboratory, Gregor Hausammann for helping with the EDML  $N_2O$  measurements, Jacqueline Flückiger for fruitful discussions, and two anonymous reviewers for helpful comments. We acknowledge financial support by the Swiss NSF and the University of Bern. This is EPICA publication no 221.

## Appendix. Supplementary data

EDC and EDML  $N_2O$  records are linked to the online version of this paper at doi:10.1016/j.quascirev.2009.03.011. The records can also be downloaded from the website of the World Data Center for Paleoclimatology at [www.ncdc.noaa.gov/paleo](http://www.ncdc.noaa.gov/paleo).

## References

- Abyzov, S.S., Mitskevich, I.N., Poglazova, M.N., 1998. Microflora of the deep glacier horizons of Central Antarctica. *Microbiology* 67, 451–458.
- Bange, H.W., Rapsomanikis, S., Andreae, M.O., 1996. Nitrous oxide emissions from the Arabian Sea. *Geophysical Research Letters* 23, 3175–3178.
- Bouwman, A.F., Funck, I., Matthews, E., John, J., 1993. Global analysis of the potential for N<sub>2</sub>O production in natural soils. *Global Biogeochemical Cycles* 7, 557–597.
- Brook, E.J., Sowers, T., Orchard, J., 1996. Rapid variations in atmospheric methane concentration during the past 110,000 Years. *Science* 273, 1087–1091.
- Dällenbach, A., Blunier, T., Flückiger, J., Stauffer, B., Chappellaz, J., Raynaud, D., 2000. Changes in the atmospheric CH<sub>4</sub> gradient between Greenland and Antarctica during the Last Glacial and the transition to the Holocene. *Geophysical Research Letters* 27, 1005–1008.
- Davidson, E.A., 1991. Fluxes of nitrous oxide and nitric oxide from terrestrial ecosystems. In: Rogers, J.E., Whitman, W.B. (Eds.), *Microbial Production and Consumption of Greenhouse Gases: Methane, Nitrogen Oxides and Halomethanes*. American Society for Microbiology, Washington, D. C.
- Enting, I.G., 1987. On the use of smoothing splines to filter CO<sub>2</sub> data. *Journal of Geophysical Research* 92, 10977–10984.
- EPICA community members, 2004. Eight glacial cycles from an Antarctic ice core. *Nature* 429, 623–628.
- EPICA community members, 2006. One-to-one coupling of glacial climate variability in Greenland and Antarctica. *Nature* 444, 195–198.
- Fischer, H., Behrens, M., Bock, M., Richter, U., Schmitt, J., Loulergue, L., Chappellaz, J., Spahni, R., Blunier, T., Leuenberger, M., Stocker, T.F., 2008. Changing boreal methane sources and constant biomass burning during the last termination. *Nature* 452, 864–867.
- Flückiger, J., Dällenbach, A., Blunier, T., Stauffer, B., Stocker, T.F., Raynaud, D., Barnola, J.M., 1999. Variations in atmospheric N<sub>2</sub>O concentration during abrupt climatic changes. *Science* 285, 227–230.
- Flückiger, J., Monnin, E., Stauffer, B., Schwander, J., Stocker, T.F., Chappellaz, J., Raynaud, D., Barnola, J.M., 2002. High-resolution Holocene N<sub>2</sub>O ice core record and its relationship with CH<sub>4</sub> and CO<sub>2</sub>. *Global Biogeochemical Cycles* 16, 1010. doi:10.1029/2001GB001417.
- Flückiger, J., Blunier, T., Stauffer, B., Chappellaz, J., Spahni, R., Kawamura, K., Schwander, J., Stocker, T.F., Dahl-Jensen, D., 2004. N<sub>2</sub>O and CH<sub>4</sub> variations during the last glacial epoch: insight into global processes. *Global Biogeochemical Cycles* 18, GB1020. doi:10.1029/2003GB002122.
- Forster, P., Ramaswamy, V., Artaxo, P., Bernsten, T., Betts, R., Fahey, D.W., Haywood, J., Lean, J., Lowe, D.C., Myhre, G., Nganga, J., Prinn, R., Raga, G., Schulz, M., Van Dorland, R., 2007. Changes in atmospheric constituents and in radiative forcing. In: Solomon, S., Qin, D., Manning, M., Chen, Z., Marquis, M., Averyt, K.B., Tignor, M., Miller, H.L. (Eds.), *Climate Change 2007: The Physical Science Basis. Contribution of Working Group I to the Fourth Assessment Report of the Intergovernmental Panel on Climate Change*. Cambridge University Press, Cambridge, United Kingdom and New York, NY, USA.
- Huber, C., Leuenberger, M., Spahni, R., Flückiger, J., Schwander, J., Stocker, T.F., Johnsen, S., Landais, A., Jouzel, J., 2006. Isotope calibrated Greenland temperature record over Marine Isotope Stage 3 and its relation to CH<sub>4</sub>. *Earth and Planetary Science Letters* 243, 504–519.
- Jouzel, J., Masson, V., Cattani, O., Falourd, S., Stievenard, M., Stenni, B., Longinelli, A., Johnsen, S.J., Steffensen, J.P., Petit, J.R., Schwander, J., Souchez, R., Barkov, N.I., 2001. A new 27 kyr high resolution East Antarctic climate record. *Geophysical Research Letters* 28, 3199–3202.
- Jouzel, J., Masson-Delmotte, V., Cattani, O., Dreyfus, G., Falourd, S., Hoffmann, G., Minster, B., Nouet, J., Barnola, J.M., Chappellaz, J., Fischer, H., Gallet, J.C., Johnsen, S., Leuenberger, M., Loulergue, L., Lüthi, D., Oerter, H., Parrenin, F., Raisbeck, G., Raynaud, D., Schilt, A., Schwander, J., Selmo, E., Souchez, R., Spahni, R., Stauffer, B., Steffensen, J.P., Stenni, B., Stocker, T.F., Tison, J.L., Werner, M., Wolff, E.W., 2007. Orbital and millennial Antarctic climate variability over the past 800,000 years. *Science* 317, 793–796.
- Köhler, P., Fischer, H., Munhoven, G., Zeebe, R.E., 2005. Quantitative interpretation of atmospheric carbon records over the last glacial termination. *Global Biogeochemical Cycles* 19, GB4020. doi:10.1029/2004GB002345.
- Kroeze, C., Mosier, A., Bouwman, L., 1999. Closing the global N<sub>2</sub>O budget: a retrospective analysis 1500–1994. *Global Biogeochemical Cycles* 13 (1), 1–8.
- Lambert, F., Delmonte, B., Petit, J.R., Bigler, M., Kaufmann, P.R., Hutterli, M.A., Stocker, T.F., Ruth, U., Steffensen, J.P., Maggi, V., 2008. Dust-climate couplings over the past 800,000 years from the EPICA Dome C ice core. *Nature* 452, 616–619.
- Lisiecki, L.E., Raymo, M.E., 2005. A Pliocene–Pleistocene stack of 57 globally distributed benthic delta O-18 records. *Paleoceanography* 20, PA1003. doi:10.1029/2004PA001071.
- Loulergue, L., Parrenin, F., Blunier, T., Barnola, J.M., Spahni, R., Schilt, A., Raisbeck, G., Chappellaz, J., 2007. New constraints on the gas age-ice age difference along the EPICA ice cores, 0–50 kyr. *Climate of the Past* 3, 527–540.
- Loulergue, L., Schilt, A., Spahni, R., Masson-Delmotte, V., Blunier, T., Lemieux, B., Barnola, J.M., Raynaud, D., Stocker, T.F., Chappellaz, J., 2008. Orbital and millennial-scale features of atmospheric CH<sub>4</sub> over the past 800,000 years. *Nature* 453, 383–386.
- Lüthi, D., Le Floch, M., Bereiter, B., Blunier, T., Barnola, J.M., Siegenthaler, U., Raynaud, D., Jouzel, J., Fischer, H., Kawamura, K., Stocker, T.F., 2008. High-resolution carbon dioxide concentration record 650,000–800,000 years before present. *Nature* 453, 379–382.
- Meissner, K.J., Galbraith, E.D., Volker, C., 2005. Denitrification under glacial and interglacial conditions: a physical approach. *Paleoceanography* 20, PA3001. doi:10.1029/2004PA001083.
- Meure, C.M., Etheridge, D., Trudinger, C., Steele, P., Langenfelds, R., van Ommen, T., Smith, A., Elkins, J., 2006. Law Dome CO<sub>2</sub>, CH<sub>4</sub> and N<sub>2</sub>O ice core records extended to 2000 years BP. *Geophysical Research Letters* 33, L14810. doi:10.1029/2006GL026152.
- Minschwaner, K., Carver, R.W., Briegleb, B.P., Roche, A.E., 1998. Infrared radiative forcing and atmospheric lifetimes of trace species based on observations from UARS. *Journal of Geophysical Research – Atmospheres* 103, 23,243–23,253.
- Miteva, V., Sowers, T., Brechley, J., 2007. Production of N<sub>2</sub>O by ammonia oxidizing bacteria at subfreezing temperatures as a model for assessing the N<sub>2</sub>O anomalies in the Vostok ice core. *Geomicrobiology Journal* 24, 451–459.
- Monnin, E., Indermühle, A., Dällenbach, A., Flückiger, J., Stauffer, B., Stocker, T.F., Raynaud, D., Barnola, J.M., 2001. Atmospheric CO<sub>2</sub> concentrations over the last glacial termination. *Science* 291, 112–114.
- Monnin, E., Steig, E.J., Siegenthaler, U., Kawamura, K., Schwander, J., Stauffer, B., Stocker, T.F., Morse, D.L., Barnola, J.M., Bellier, B., Raynaud, D., Fischer, H., 2004. Evidence for substantial accumulation rate variability in Antarctica during the Holocene, through synchronization of CO<sub>2</sub> in the Taylor Dome, Dome C and DML ice cores. *Earth and Planetary Science Letters* 224, 45–54.
- Nevison, C.D., Weiss, R.F., Erickson, D.J., 1995. Global oceanic emissions of nitrous oxide. *Journal of Geophysical Research – Oceans* 100, 15809–15820.
- Parrenin, F., Barnola, J.M., Beer, J., Blunier, T., Castellano, E., Chappellaz, J., Dreyfus, G., Fischer, H., Fujita, S., Jouzel, J., Kawamura, K., Lemieux-Dudon, B., Loulergue, L., Masson-Delmotte, V., Narcisi, B., Petit, J.R., Raisbeck, G., Raynaud, D., Ruth, U., Schwander, J., Severi, M., Spahni, R., Steffensen, J.P., Svensson, A., Udisti, R., Waelbroeck, C., Wolff, E., 2007. The EDC3 chronology for the EPICA Dome C ice core. *Climate of the Past* 3, 485–497.
- Petit, J.R., Jouzel, J., Raynaud, D., Barkov, N.I., Barnola, J.M., Basile, I., Bender, M., Chappellaz, J., Davis, M., Delaygue, G., Delmotte, M., Kotlyakov, V.M., Legrand, M., Lipenkov, V.Y., Lorius, C., Pepin, L., Ritz, C., Saltzman, E., Stievenard, M., 1999. Climate and atmospheric history of the past 420,000 years from the Vostok ice core, Antarctica. *Nature* 399, 429–436.
- Potter, C.S., Matson, P.A., Vitousek, P.M., Davidson, E.A., 1996. Process modeling of controls on nitrogen trace gas emissions from soils worldwide. *Journal of Geophysical Research – Atmospheres* 101, 1361–1377.
- Rohde, R.A., Price, P.B., Bay, R.C., Bramall, N.E., 2008. In situ microbial metabolism as a cause of gas anomalies in ice. *Proceedings of the National Academy of Sciences of the United States of America* 105, 8667–8672.
- Schmittner, A., Galbraith, E.D., 2008. Glacial greenhouse-gas fluctuations controlled by ocean circulation changes. *Nature* 456, 373–376.
- Siegenthaler, U., Stocker, T.F., Monnin, E., Lüthi, D., Schwander, J., Stauffer, B., Raynaud, D., Barnola, J.M., Fischer, H., Masson-Delmotte, V., Jouzel, J., 2005. Stable carbon cycle-climate relationship during the late Pleistocene. *Science* 310, 1313–1317.
- Sowers, T., 2001. N<sub>2</sub>O record spanning the penultimate deglaciation from the Vostok ice core. *Journal of Geophysical Research – Atmospheres* 106, 31903–31914.
- Spahni, R., Schwander, J., Flückiger, J., Stauffer, B., Chappellaz, J., Raynaud, D., 2003. The attenuation of fast atmospheric CH<sub>4</sub> variations recorded in polar ice cores. *Geophysical Research Letters* 30, 1571. doi:10.1029/2003GL017093.
- Spahni, R., Chappellaz, J., Stocker, T.F., Loulergue, L., Hausammann, G., Kawamura, K., Flückiger, J., Schwander, J., Raynaud, D., Masson-Delmotte, V., Jouzel, J., 2005. Atmospheric methane and nitrous oxide of the late Pleistocene from Antarctic ice cores. *Science* 310, 1317–1321.
- Stauffer, B., Flückiger, J., Monnin, E., Schwander, J., Barnola, J.M., Chappellaz, J., 2002. Atmospheric CO<sub>2</sub>, CH<sub>4</sub> and N<sub>2</sub>O records over the past 60,000 years based on the comparison of different polar ice cores. *Annals of Glaciology* 35, 202–208.
- Stocker, T.F., 1998. Climate change – the seesaw effect. *Science* 282, 61–62.
- Stocker, T.F., Johnsen, S.J., 2003. A minimum thermodynamic model for the bipolar seesaw. *Paleoceanography* 18, 1087. doi:10.1029/2003PA00092.
- Volk, C.M., Elkins, J.W., Fahey, D.W., Dutton, G.S., Gilligan, J.M., Loewenstein, M., Podolske, J.R., Chan, K.R., Gunson, M.R., 1997. Evaluation of source gas lifetimes from stratospheric observations. *Journal of Geophysical Research – Atmospheres* 102, 25543–25564.
- Watson, A.J., Garabato, A.C.N., 2006. The role of Southern Ocean mixing and upwelling in glacial-interglacial atmospheric CO<sub>2</sub> change. *Tellus Series B* 58, 73–87.